Journal of Macromolecular Science, Part A
Publication details, including instructions for authors and subscription information:
http://www.informaworld.com/smpp/title~content=t713597274

Particle Formation in Emulsion Polymerization: Transient Particle Concentration

Zhigiang Song[a]; Gary W. Poehlein[a]
[a] School of Chemical Engineering Georgia Institute of Technology, Atlanta, Georgia

To cite this Article Song, Zhigiang and Poehlein, Gary W.(1988) 'Particle Formation in Emulsion Polymerization: Transient Particle Concentration', Journal of Macromolecular Science, Part A, 25: 4, 403 — 443
To link to this Article: DOI: 10.1080/00222338808053377
URL: http://dx.doi.org/10.1080/00222338808053377

J. MACROMOL. SCI.—CHEM., A25(4), pp. 403-443 (1988)

PARTICLE FORMATION IN EMULSION POLYMERIZATION: TRANSIENT PARTICLE CONCENTRATION

ZHIGIANG SONG and GARY W. POEHLEIN

School of Chemical Engineering
Georgia Institute of Technology
Atlanta, Georgia 30332-0100

ABSTRACT

A general kinetic model of particle formation in emulsion polymerization is presented. This model takes into account homogeneous, micellar, and monomer droplet nucleation mechanisms. Chain transfer and termination in the aqueous phase, capture of oligomer radicals by particles, and coagulation of particles are also considered. A three-parameter analytical solution is obtained for the transient particle consideration:

$$\frac{N}{N_s} = \frac{1 - e^{-t/\tau}}{1 + (1/A_2)e^{-t/\tau}},$$

where N and N_s are particle concentrations in number per volume of aqueous phase during the nucleation period and at steady state, respectively; t is time; and A_2 and τ are adjustable model parameters. The model parameters N_s, A_2, and τ can be estimated from basic kinetic parameters and reaction conditions. Model predictions are in agreement with experimental data obtained from the literature. Values of the average rate coefficient for coagulation obtained from fitting the model to the experimental data were used to calculate the coagulation-average particle diameter. These coagulation-average particle diameters are much less than the measured particle diameters because small particles have a much stronger tendency to coagulate than large particles.

INTRODUCTION

Quantitative prediction of the number of particles formed and stabilized is a central problem in emulsion polymerization kinetics. Harkins [1, 2] was the first to propose a nucleation mechanism based on free radical penetration into monomer-swollen emulsifier micelles. Smith and Ewart [3, 4] developed a mathematical model based on this mechanism and particle growth kinetics. This treatment, which is known as the Smith-Ewart Case 2 model, predicts that the number of particles at the end of the nucleation period, Interval I, will be proportional to the 0.4 power of initiation rate ρ_i and the 0.6 power of emulsifier concentration S, i.e.,

$$N_S = K(\rho_i/\mu)^{0.4}(a_s S)^{0.6}, \tag{1}$$

where K is a constant with a value between 0.37 and 0.53; μ is the rate of volume increase of a polymer particle for S-E Case 2 kinetics, and a_s is the interfacial area that can be covered by a unit weight of emulsifier. This theory is applicable to sparingly water-soluble monomers, such as styrene.

Priest [5], on the other hand, established the main concepts of the homogeneous nucleation mechanism. Fitch [6-8] put these concepts in the methematical form

$$dN/dt = b\rho_i - R_c - R_i, \tag{2}$$

where t is time, b is a constant introduced to account for the aggregation of radicals, R_c is the rate at which radicals are captured by particles, and R_f is the coagulation rate among particles. This equation was treated quantitatively by Hansen and Ugelstad [9-12]. Thus, the homogeneous nucleation theory, parallel to the Smith-Ewart theory for sparingly water-soluble monomers, became the prevailing theory for more water-soluble monomer such as methyl methacrylate and vinyl acetate.

Although the Smith-Ewart theory and the homogeneous nucleation theory are successful for some systems, neither of them alone is consistent with all the experimental facts. Using mixed surfactants in the emulsion polymerization of styrene, Kamath [13] believed that the particle nucleation mechanism followed the Smith-Ewart theory. Piirma [14], however, noticed that Kamath's data and her own experimental results did not generate a straight line on a plot of log R_p against log S as is predicted by Eq. (1) for constant a_s. To explain this, she proposed and showed that micellar size must be considered in particle nucleation during emulsion polymeriza-

tion. Before Piirma, Roe [15] observed that the total number of particles generated depends on the composition of the mixed surfactant and not on the total number of micelles. Nakagawa and Kuryana et al. [16, 17] confirmed the concepts of micelle formation by mixed surfactant systems. Wood et al. [18] found that the size of polystyrene particles decreased with increasing amount of the ionic component in the surfactant mixtures. Thus, they proposed that the larger polystyrene particles came from the larger miscelles.

To test whether the parameter a_s appearing in Eq. (1) of the Smith-Ewart theory could account for the micelle size effects mentioned above, Dunn et al. [19, 20] carried out experiments with two series of alkyl carboxylates and alkyl sulfates as emulsifiers. Values of a_s of the former series decrease with increasing alkyl chain length, while the molecules of latter series has approximately the same a_s values. They found that equal concentrations of micellar emulsifier gave equal numbers of latex particles with the same particle size distribution and the same Interval II polymerization rate. The duration of Interval I, however, varied with different emulsifiers used. Consequently, they suggested that the surface area of the original micelles (not a_s) might be the factor which determines the number of latex particles ultimately formed.

Interval I, particle nucleation, first proposed by Harkins, was generally believed to end at about 10-15% or less conversion [21]. Such a short period of nucleation can be calculated with the Smith-Ewart theory, which assumes that polymer particle nucleation ends with the disappearance of the micelles. This has been tested by Smith [4] and others [22] using high monomer (styrene)/water (M/W) ratios (40/60-30/70). However, at a low M/W ratio (10/90), Chatterjee [23-25] and Robb [26] found that N increased continuously up to 35-40% conversion. This might be consistent with the Smith-Ewart theory if the same amount of the emulsifier were used and similar sizes of polymer particles were produced. The same number of polymer particles can be saturated by emulsifier, and this saturation will occur at higher monomer conversion for lower M/W ratio recipes. Alexander and Napper [21] reexamined the data reported by Van der Hoff [27] for high M/W ratios in styrene emulsion polymerization and found that the particle number increased linearly with conversion up to 40%. Zollars [28] has even reported, for the emulsion polymerization of vinyl acetate, that particle concentration increased with conversion from 11 to 95%. All this evidence of a prolonged Interval I emphasizes the significance of studying particle nucleation in emulsion polymerization.

In addition to micelle entry and homogeneous nucleation, Ugelstad et al. [10, 29, 30] and Durlin et al. [31] clearly demonstrated that monomer drop-

lets can be a significant locus for particle formation if the droplets are made small enough. Poehlein [32] showed that polymer particles are likely to be formed from droplets even if they are as large as 5-10 μm. Lichti et al. [34] and Feeney et al. [34, 35] observed in recent papers that the rate of production of new latex particles increased during much of the nucleation period in the emulsion polymerization of styrene. To explain this, they proposed a two-step coagulative nucleation model.

It is evident from the facts mentioned above that there are three loci for particle nucleation: 1) monomer-swollen micelles, 2) aqueous phase, and 3) monomer droplets. All three loci of particle nucleation are possible in an emulsion polymerization system. Which mechanism is more important in a system depends on the specifics of that system and the conditions under which the emulsion polymerization is carried out. While aqueous phase nucleation can occur in emulsion polymerization under any conditions, micelle-entry nucleation requires the existence of micelles and, therefore, a concentration of emulsifier above the critical micelle concentration (CMC). Monomer droplet nucleation requires the existence of the separated monomer phase and is enhanced by an increased total surface area of the monomer droplets.

Monomer solubility in water plays an important role in nucleation phenomena. With sparingly water-soluble monomer such as styrene, monomer-swollen micelles are thought to be the main locus, and many workers completely ignore monomer deoplet and homogeneous nucleation in these systems. Similarly, the micelle nucleation mechanism can play an important part in polymerization of more water-soluble monomers, such as methyl methacrylate and vinyl acetate, provided that the concentration of emulsifier is far above the CMC.

The fact that both micelle entry and homogeneous nucleation occur in a system was clearly demonstrated by Sutterlin et al. [36, 37]. They investigated particle formation with a series of acrylates and methacrylates. The S-shaped curves of particle number versus emulsifier concentration differed for different monomers. With sparingly water-soluble monomers, the deflection of the curves at the CMC was clearly evident; with more water-soluble monomers, the change in the slope of the curves at the CMC was less pronounced. Hansen and Ugelstad [11] carried out seeded and unseeded polymerizations with styrene using sodium dodecyl sulfate as emulsifier, to test if both micelle-entry and homogeneous nucleation occur in such systems. They concluded that, while the homogeneous nucleation mechanism predominated when the concentration of emulsifier was below the CMC, micelles became the dominating loci for particle nucleation when the concentration of emulsifier was above the CMC.

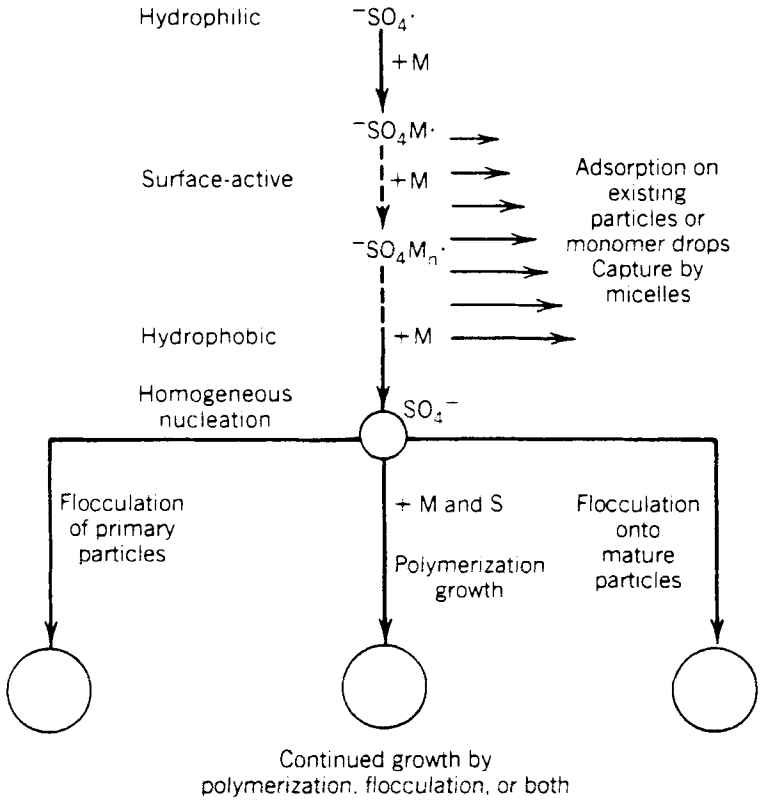

FIG. 1. Paths for water-initiated free radicals. M = monomer; S = surfactant.

No theory has been published which includes all three particle nucleation mechanisms in a methematical model. Nevertheless, Poehlein [38] has summarized previous work and proposed a comprehensive picture of mechanisms for particle nucleation, as shown in Fig. 1. Poehlein's scheme includes all three particle nucleation mechanisms in a persulfate-initiated emulsion polymerization system. Poehlein has further pointed out that a transfer radical which has desorbed from a particle into the aqueous phase will also take the paths as shown in Fig. 1 for an initiator radical. In this paper a mathematical model is developed based on Poehlein's scheme of particle nucleation. An equation similar in form to Eq. (2) given by Fitch [6-8] is derived. An analytical solution of this equation is obtained which permits one to predict the transient behavior of particle nucleation in emulsion polymerization. The theoreti-

cal predictions are in agreement with experimental data taken from literature.

GENERAL PARTICLE NUCLEATION MECHANISM

The mathematical model presented in this paper follows the particle nucleation scheme proposed by Poehlein [38] (Fig. 1). An emulsion polymerization system in which there exist monomer droplets and micelles in the continuous aqueous phase is considered. The free radicals formed in the aqueous phase may 1) add monomeric units dissolved in the water; 2) be absorbed (after adding at least one monomer unit) into monomer-swollen micelles; 3) be absorbed into monomer droplets; 4) be captured by the existing polymer particles; 5) terminate in the aqueous phase; or 6) lose activity by chain transfer to another species.

A primary radical formed from water-soluble initiator is not likely to be absorbed directly by monomer-swollen micelles or monomer droplets because of its hydrophilic nature and charge. Once monomeric units are added, however, it becomes an oligomeric free radical and its hydrophobicity is increased so that the tendency to be absorbed directly by monomer-swollen micelles, monomer droplets, or existing monomer-swollen polymer particles increases greatly. A primary radical produced by chain transfer to monomer or by thermal initiation of the monomer is different from a primary water-soluble initiator radical in that the former is hydrophobic in nature and may be captured by micelles, monomer droplets, or existing particles. If, while growing, an oligomer radical is not absorbed by the said three species, it will reach a critical chain length n^* and precipitate from the aqueous solution as a primary polymer particle. This is called homogeneous nucleation.

Primary particles precipitated by homogeneous nucleation are likely to be unstable and tend to coagulate with each other or with the existing latex particles because f their small size and lack of sufficient surfactant molecules. The parimary particles can grow simultaneously both by coagulation and by polymerization. As they are growing, they may adsorb more and more surfactant molecules and become relatively stable. Primary particles may also coagulate with, or rather be captured by, mature lates particles. However, during the initial period of polymerization when there is sufficient surfactant for stabilizing polymer particles, this tendency is less strong than that of coagulation between primary particles themselves. After the surfactant is exhausted, its surface coverage on polymer particles decreases as a result of particle growth. This tendency leads to a situation in which latex particle-

primary particle coagulation events are favored over those between two primary particles. Eventually, all primary particles being formed by homogeneous nucleation will be captured by the existing latex particles. Since micelles disappear before the exhaustion of surfactant in the aqueous phase, no micelle-entry nucleation is possible in this stage.

If no monomer droplets exist in the system, or if particle nucleation from this source is negligible, no new polymer particles will be formed in this stage. Thus, the latex particle number will remain constant at a steady-state value. Coagulation between mature latex particles is also possible. However, if the number of latex particles is reduced from such coagulation, the remaining particles may not be able to capture all free radicals, and homogeneous nucleation of primary particles may again occur in the aqueous phase. New polymer particles that are formed compensate for the loss of latex particle number from coagulation and thus tend to maintain a steady state. Primary particles nucleated from micelles are different from those formed by homogeneous nucleation due to the excess of surfactant on their surface. As a result, they are less likely to undergo coagulation and more likely to grow by polymerization.

Particles nucleated from monomer droplets are likely to be initially stable because of surfactant on the surface and adequate agitation. Once oligomer radicals enter a monomer droplet and continue to grow there, the properties of this monomer droplet, now a polymer particle, are changed. First, since the droplet now contains polymer, there is a problem of monomer partition with the aqueous phase. The volume fraction of polymer in this droplet is small at first, and there is large excess of monomer compared to the monomer content of mature polymer particles, which are closer to equilibrium with the aqueous phase. Thermodynamic forces will tend to drive this excessive monomer out of the droplet. However, the monomer concentration in the aqueous phase is kept nearly constant by transfer from the monomer droplets at about the level of monomer solubility in water. Mass transfer of this excess monomer to the aqueous phase is, therefore, limited. Thermodynamic forces will cause transport of the excess monomer out of the droplet, and shear forces in agitated systems are likely to split larger droplets to affect size reduction. The larger the monomer droplets, the more unstable the primary polymer particles nucleated from them. This may explain why latex particles as large as monomer droplets are rarely observed in conventional emulsion polymerization with large monomer/water ratios in which the probability of monomer droplet nucleation may be relatively high.

When mixed surfactants are used to make monomer droplets smaller, one can easily observe the monomer-droplet-nucleated polymer particles in the

final products of emulsion polymerization [29-31, 39]. This is not only because the reduction in size of monomer droplets increases the probability of monomer droplet nucleation, but also because the reduced size of monomer droplets increases the stability of polymer particles nucleated from them.

The rate of particle coagulation depends on, among other things, the size of polymer particles. So does the rate of free-radical capture by polymer particles. It has been shown by Dunn [4] that efficiency of initiation increases with decreasing particle size. For the small particles, according to his report, the efficiency of initiation could be up to 100%. Therefore, primary particles grow quickly, more by coagulation with each other and capture of oligomeric radicals from the aqueous phase than by polymerization. It is obvious that primary particles nucleated from different sources (i.e., micelles, monomer droplets, and aqueous solution) should have different abilities to capture radicals from the aqueous phase because of their different size and different surface characteristics. It should be noted that absorption of free radical by particles could be reversible, and desorbed radicals may be recaptured by particles, micelles, or droplets.

In addition to nucleating polymer particles, free radicals in the aqueous phase may also terminate with each other or undergo chain transfer reactions. These effects will certainly influence the efficiency of particle nucleation. Solubility of monomer in water is an important factor for aqueous phase termination of free radicals. High monomer concentration in the aqueous phase favors the propagation reaction, thus decreasing the probability of aqueous phase termination. On the other hand, higher monomer solubility in water is often associated with the large critical chain length n^* of the polymer. Thus, the life of oligomeric radicals will be longer before they reach the critical size, provided that the propagation rate constant k_p is unchanged. This will obviously increase the probability of aqueous-phase termination. Very often, the latter effect is more significant.

When two oligomeric radicals terminate by combination, the oligomer produced may exceed the critical chain length n^* and precipitate from the aqueous phase as an inactive primary particle. Presumably, such particle nucleation from aqueous phase termination can be neglected compared to other kinds of particle nucleation since the concentration of oligomeric radicals in the aqueous phase is small. The oligomers generated from aqueous-phase termination can act as surfactant, because of hydrophilic end groups from the initiator, and even form micelles when the concentration is above the CMC. This effect will enhance particle nucleation. Vanderhoff [41] suggested that particle nucleation in emulsifier-free emulsion polymerization of a sparingly water-soluble monomer, such as styrene, results primarily from this micellization effect.

The effect of chain transfer in the aqueous phase will, as a whole, decrease the rate of particle nucleation. Chain transfer will prolong the average time for a primary radical to grow to the critical chain length of the polymer for homogeneous nucleation. Hydrophilic-lipophilic properties of the chain transfer agents (CTA) will also be important for micelle entry and monomer droplet entry nucleations. A hydrophilic CTA primary radical produced by chain transfer, like an initiator radical, will add monomeric units before it is able to enter a micelle or a monomer droplet for particle nucleation. As a result, the rate of particle nucleation could be reduced. On the other hand, chain transfer from oligomeric radicals to monomer, which can be considered as a lipophilic CTA, should have little influence on micelle or monomer droplet entry though it would reduce the homogeneous nucleation rate. Chain transfer from hydrophilic initiator primary radicals increases the lipophilic property of radicals and, therefore, will probably increase the rate of micelle and monomer droplet entry nucleation but reduce the rate of homogeneous nucleation.

Chain transfer reactions in the particle phase have different effects from those in the aqueous phase. Chain transfer between polymer radicals and monomer or other low molecular weight CTA favors radical desorption from particles because of the higher mobility of the low molecular weight radicals. The desorbed radicals can take the same paths for initiator radicals, as shown in Fig. 1. That is, the desorbed radicals may be reabsorbed by particles, enter micelles or monomer droplets, grow to the critical size and precipitate from the aqueous phase, terminate with other radicals, or transfer their activity to other species in the aqueous phase. Thus, chain transfer in the particle phase will enhance particle nucleation.

Besides being a locus of particle nucleation, micelles also serve as a surfactant reservoirs in the system. The concentration of surfactant in the aqueous solution will be kept nearly constant until the disappearance of micelles. Similarly, monomer droplets function as a monomer reservoir to maintain a nearly constant concentration of monomer in the aqueous phase and also maintain thermodynamic equilibrium of monomer between the aqueous phase and polymer phase.

The general particle nucleation mechanism presented above can be expressed by the following chemical and physical processes ("reactions").

1.	$I \xrightarrow{k_d} 2R^{\cdot}$		Initiation
2.	$R^{\cdot} + M \xrightarrow[(k_{ia})]{k_i} M_1$		Competition for primary radicals from initiator ($R^{\cdot}$) or from chain transfer agent ($A^{\cdot}$)
3.	(or $A^{\cdot}$) $Mc \xrightarrow{k_{ic}} Mc \longrightarrow Pc_1$		
4.	$Md \xrightarrow{k_{id}} Md \longrightarrow Pd_1$		
5.	$M_i \xrightarrow{k_{ti}} O_i$		
6.	$P_i \xrightarrow{k_{ci}} P_{i+1}$		
7.	$R^{\cdot} + CTA \xrightarrow{k_{tr}} A^{\cdot}$		Chain transfer from $R^{\cdot}$ to CTA
8.	$M_i + M \xrightarrow{k_p} M_{i+1} \xrightarrow{i+1=n^*} Pa_1$	$i = 1, 2, \ldots, (n^* - 1)$	Propagation or homogeneous nucleation
9.	$Mc \xrightarrow{K_{mc}} Mc \longrightarrow Pc_1$		Micelle entry nucleation
10.	$Md \xrightarrow{K_{md}} Md \longrightarrow Pd_1$		Monomer droplet nucleation
11.	$M_j \xrightarrow{k_{tw}} M_{j+i} \xrightarrow{i+j \geq n^*} Pa_1$		Aqueous phase termination
12.	$P_j \xrightarrow{K_{cj}} P_{j+1}, (j = 1, 2, \ldots)$		Radical capture by particles
13.	$CTA \xrightarrow{k_{tr}} A^{\cdot} + O_i$		Chain transfer to CTA
14.	$\dot{M} \xrightarrow{k_{trm}} M_1 + O_i$		Chain transfer to monomer

15. $P \xrightarrow{K_{ei}} P + M_i$ — Radical desorption from particles

16. $P_i + P_j \xrightarrow{K_{fij}} P_{i+j}$ $i = 1, 2, \ldots$ $j = 1, 2, \ldots$ — Particle coagulation

17. $Mc + P \xrightarrow{R_{mp}} P$ — Micelle disappearance to cover newly formed particle surface

18. $Md + Md \underset{R_{md}''}{\overset{R_{mp}'}{\rightleftharpoons}} Md$ — Monomer droplet coalescence and separation

where the symbols used are defined in the Symbols section preceding the references.

MATHEMATICAL MODELS

Before model equations are established for particle nucleation, the following assumptions based on the analysis in the previous part are utilized.

(1) Reactions 3-6 are negligible compared to Reaction 2 because of the hydrophilic nature of the primary radical $R^{\bullet}$ (or CTA radical $A^{\bullet}$).
(2) Once an oligomeric radical enters a micelle or monomer droplet, the latter becomes a primary polymer particle. This means that the last step in Reaction 9 and Reaction 10 is much faster than the former step, i.e., polymerization (propagation) inside the particles is much faster than the rate of radical absorption by micelles or monomer droplets in the aqueous phase.
(3) The reversible effects (K_{mc}'' and K_{md}'') in Reactions 9 and 10 can be taken into account by adding correction factors (F_c and F_d, respectively) in the corresponding positive reaction rate constants (K_{mc}' and K_{md}'). Thus, let $K_{mc} = F_c K_{mc}'$ and $K_{md} = F_d K_{md}'$.

Balance equations of the model subject to these assumptions are as follows.

The total polymer particle formation rate

$$(1/N_A)\,dN/dt = d[P]/dt = k_p M_w [M_{n^*-1}] + K_{mc}[Mc][R_w] + K_{md}[Md][R_w] - (1/2)\sum_{i=1}^{\infty}\sum_{j=1}^{\infty} K_{f_{ij}}[P_i][P_j] - (1/2)\sum_{i=1}^{\infty} K_{f_{ii}}[P_i]^2 + k_{tw}\sum_{i=1}^{n^*-1}\sum_{k=1}^{i} [M_i][M_{n^*-k}]. \quad (3)$$

The formation rate of particles of Class 1, $[P_1]$

$$(1/N_A)\,dN_1/dt = d[P_1]/dt = k_p M_w [M_{n^*-1}] + K_{mc}[Mc][R_w] + K_{md}[Md][R_w] - \sum_{j=1}^{\infty} K_{f_{ij}}[P_1][P_j] - K_c[P_1][R_w] + k_{tw}\sum_{i=1}^{n^*-1}\sum_{k=1}^{i} [M_i][M_{n^*-k}]. \quad (4)$$

The formation rate of particles of Class i, $[P_i]$

$$(1/N_A)\,dN_i/dt = d[P_i]/dt = (1/2)\sum_{j=1}^{i-1} K_{f_{i-1,j}}[P_j][P_{i-j}] - \sum_{j=1}^{\infty} K_{f_{ij}}[P_i][P_j] - (1/2)K_{f_{i-1,i-1}}[P_{i-1}]^2 + K_{c_{i-1}}[P_{i-1}][R_w] - K_{c_i}[P_i][R_w] \quad (i = 2, 3, \ldots). \quad (5)$$

The rate of disappearance of micelles

$$-d[Mc]/dt = K_{mc}[R_w][Mc] + R_{mc}. \quad (6)$$

The rate of disappearance of monomer droplets

$$-d[Md]/dt = K_{md}[R_w][Md] + R_{md}' - R_{md}''. \quad (7)$$

Formation rate for the 1st oligomeric radicals in the aqueous phase

$$d[M_1]/dt = \rho_i + K_{e_1}[Pm_1] - k_p M_w [M_1] - K_{mc}[MC][M_1] - K_{md}[Md][M_1] - \sum_{j=1}^{\infty} K_{c_j}[P_j][M_1] - k_{tr}[CTA]_w[M_1] + k_{trm}[M][R_w] + k_{ia}[A^*]M_w - k_{tw}([M_1]^2 + \sum_{j=1}^{n^*-1}[M_1][M_j]). \quad (8)$$

Formation rate for ith oligomeric radicals in the aqueous phase

$$d[M_i]/dt = k_p M_w [M_{i-1}] + K_{e_i}[Pm_i] - k_p M_w [M_i] - K_{mc}[Mc][M_i] - K_{md}[M_i][Md] - \sum_{j=1}^{\infty} K_{c_j}[P_j][M_1] - k_{tr}[M_i][CTA]_w - k_{trm}[M_i]M_w - k_{tw}[M_i]([M_i] + \sum_{j=1}^{n^*-1}[M_j]) \quad (i = 2, 3, \ldots). \quad (9)$$

Formation rate of total oligomer radicals in the aqueous phase,

$$[R_w] = \sum_{j=1}^{n^*-1}[M_j]$$

$$d[R_w]/dt = \rho_i + \sum_{i=1}^{n^*-1} K_{e_i}[Pm_i] - k_p M_w [M_{n^*-1}] - K_c[Mc][R_w] - K_{md}[Md][R_w] - \sum_{j=1}^{\infty} K_{c_j}[P_j][R_w] - k_{tw}[R_w] - k_{tw}\sum_{j=1}^{\infty}[M_i]^2 - k_{tr}[CTA]_w[R_w] + k_{ia}[A^*]M_w. \quad (10)$$

Disappearance rate of the chain transfer agent CTA

$$-d[CTA]_w/dt = k_{tr}[CTA]_w[R_w]. \quad (11)$$

Formation rate of CTA radicals

$$d[A^{\cdot}]/dt = k_{tr}[CTA]_w[R_w] - k_{ia}[A^{\cdot}]M_w \tag{12}$$

where symbols of species in square brackets [ ] represent the concentration of the bracketed species in mol/L. $[Pm_i]$ is the concentration of particles which contain polymer radicals with chain length i, ($i = 1, 2, \ldots$). K_e represents the rate constant for desorption of the radicals with chain length i from the particle phase.

In principle, relationships for $[P_j]$-t, [Mc]-t, [Md]-t, $[CTA]_w$-t, $[M_i]$-t, and $[A^{\cdot}]$-t can be obtained by solving the above simultaneous differential equations provided that all parameters and the monomer solubility in water are known. Solution of the complete model is difficult for a variety of reasons. To simplify the problem, the following further assumptions are used.

(4) Steady state of all radical concentrations in the aqueous phase.
(5) The terms $k_{tw}[M_i]^2$, ($i = 1, 2, 3, \ldots$), in Eqs, (8), (9), and (10) can be neglected, since $[M_i]$ is much smaller than $\sum_{i=1}^{n^*-1} [M_i]$.

The following relationships for $[M_1]$ and $[M_i]$ are obtained from Eqs. (8) and (9) with the use of Assumptions (4) and (5).

$$[M_1] = \frac{\rho_i + k_{ia}[A^{\cdot}][M] + k_{trm}M_w[R_w] + K_{e_i}[Pm_1]}{k_pM_w + K_{mc}[Mc] + K_{md}[Md] + k_{tw}[R_w] + k_{tr}[CTA]_w + k_{trm}M_w + K_c[P]}, \tag{13}$$

$$[M_i] = \frac{k_pM_w[M_{i-1}] + K_{e_i}[Pm_i]}{k_pM_w + K_{mc}[Mc] + K_{md}[Md] + k_{tw}[R_w] + k_{tr}[CTA]_w + k_{trm}M_w + K_c[P]}$$

($i = 2, 3, 4, \ldots, n^* - 1$). (14)

The following definitions are used to simplify symbols. Total radical concentration in the aqueous phase

$$[R_w] = \sum_{i=1}^{n^*-1} [M_i]. \tag{15}$$

Total desorption rate of radicals from particles

$$\rho_e = \sum_{i=1}^{n^*-1} K_{e_i}[\mathrm{Pm}_i]. \tag{16}$$

Desorption rate of radicals with chain length i,

$$\rho_{ei} = K_{e_i}[\mathrm{Pm}_i]. \tag{17}$$

The rate of reinitiation by chain transfer agent radicals using Assumption 4 for $d[\mathrm{A}^\cdot]/dt = 0$

$$\rho_{ia} = k_{ia}[\mathrm{A}^\cdot]\mathrm{M}_w = k_{tr}[\mathrm{CTA}]_w[\mathrm{R}_w]. \tag{18}$$

The rate of chain transfer to monomer

$$\rho_{im} = k_{trm}\mathrm{M}_w[\mathrm{R}_w]. \tag{19}$$

Let

$$\rho = \rho_i + \rho_{ia} + \rho_{im}. \tag{20}$$

The average rate constant of radical capture by particles

$$K_c \frac{\sum_{i=1}^{\infty} K_{c_i}[\mathrm{P}_i]}{[\mathrm{P}]}. \tag{21}$$

The average coagulation rate constant for particles

$$K_f = \frac{(1/2)\sum_{i=1}^{\infty}\sum_{j=1}^{\infty} K_{f_{ij}}[\mathrm{P}_i][\mathrm{P}_j] + (1/2)\sum_{i=1}^{\infty}[\mathrm{P}_i]^2}{[\mathrm{P}]^2}. \tag{22}$$

The average rate constant of radical desorption from particles

$$K_e = \frac{\sum_{i=1}^{n^*-1} K_{e_i}[\mathrm{Pm}_i]}{\bar{n}[\mathrm{P}]}. \tag{23}$$

The probability for an oligomeric radical to propagate

$$\alpha_p = \frac{k_p M_w}{k_p M_w + K_{mc}[Mc] + K_{md}[Md] + k_{tw}[R_w] + k_{tr}[CTA]_w + k_{trm} M_w + K_c[P]} \tag{24}$$

The desorption parameter

$$\gamma = K_e/(k_p M_w) \tag{25}$$

Equations (13) and (14) can then be rewritten as

$$[M_1] = \alpha_p \rho/k_p M_w) + \alpha_p \gamma [Pm_1], \tag{26}$$

$$\begin{aligned}[M_i] &= \alpha_p [M_{i-1}] + \alpha_p \gamma [Pm_i] \\ &= \alpha_p(\alpha_p [M_{i-2}] + \alpha_p \gamma [Pm_{i-1}]) + \alpha_p \gamma [Pm_i] \\ &= \alpha_p^{i-1} [M_1] + \gamma \alpha_p^{i-1} [Pm_2] + \gamma \alpha^{i-2} [Pm_3] + \cdots + \alpha_p \gamma [Pm_i]. \end{aligned} \tag{27}$$

Substituting Eq. (26) into Eq. (27) gives

$$[M_i] = \alpha_p^{\,i} \rho/(k_p M_w) + \sum_{j=0}^{i-1} \gamma \alpha_p^{\,i+1} [Pm_{i-j}]. \tag{28}$$

The total radical concentration in the aqueous phase is then

$$\begin{aligned}[R_w] &= \sum_{i=1}^{n^*-1} \alpha_p^{\,i} \rho/(k_p M_w) + \sum_{i=0}^{n^*-1} \left(\sum_{j=0}^{i-1} \gamma \alpha_p^{\,j+1} [Pm_{i-j}] \right) \\ &= \frac{\alpha_p(1 - \alpha_p^{\,n^*-1})\rho}{(1 - \alpha_p) k_p M_w} + \sum_{i=0}^{n^*-1} \sum_{j=0}^{i-1} \gamma \alpha_p^{\,i+j} [Pm_{i-j}]. \end{aligned} \tag{29}$$

$[Pm_i]$ must be known to use Eqs. (28) and (29) in Eq. (3) for total particle concentration. $[Pm_i]$ involves the molecular weight distribution of living polymer in particles. To simplify the problem, we introduce the average number of radicals with chain length i per particle, $\bar{m}_i$. Then,

$$[Pm_i] = \bar{m}_i [P]. \tag{30}$$

Substituting Eq. (30) into Eqs. (28) and (29) yields, respectively,

$$[M_i] = \alpha_p{}^i \rho/(k_p M_w) + \gamma_i [P], \tag{31}$$

$$[R_w] = \frac{\alpha_p(1 - \alpha_p{}^{n^*-1})\rho}{(1 - \alpha_p)k_p M_w} + \gamma_t [P] = B\rho + \gamma_t [P], \tag{32}$$

where

$$\gamma_i = \sum_{j=0}^{i-1} \gamma \alpha_p{}^{i+j} \bar{m}_{i-j}, \tag{33}$$

$$\gamma_t = \sum_{i=1}^{n^*-1} \gamma_i = \sum_{i=1}^{n^*-1} \sum_{j=0}^{i-1} \gamma \alpha_p{}^{j+1} \bar{m}_{i-j}, \tag{34}$$

$$B = \frac{\alpha_p(1 - \alpha_p{}^{n^*-1})}{(1 - \alpha_p)k_p M_w}. \tag{35}$$

Substituting Eqs. (31) and (32) into Eq. (3) and rearranging yields (see the Appendix for the derivations of Eqs. 36 and 37)

$$\begin{aligned}\frac{d[P]}{dt} = {} & \left\{ \rho_i \alpha_p{}^{n^*-1} + \rho_i(1 - \alpha_p{}^{n^*-1}) + Ck_{tw}B^2\rho^2 - K_c B\rho[P] \right. \\ & \left. - k_{tw}B^2\rho^2 - K_f[P]^2 \right\} + \left\{ k_p M_w \gamma_a [P] - k_{tw}\gamma_t{}^2 [P]^2 - 2k_{tw}B\rho\gamma_t [P] \right. \\ & + [k_{tw}[P]\rho/(k_p M_w)] \sum_{i=1}^{n^*-1} \sum_{j=1}^{i} (\gamma_i \alpha_p{}^{n^*-j} + \gamma_{n^*-j}\alpha_p{}^i) \\ & \left. + k_{tw}[P]^2 \sum_{i=1}^{n^*-1} \sum_{j=1}^{i} \gamma_i \gamma_{n^*-j} \right\},\end{aligned} \tag{36}$$

where B is defined by Eq. (35) and C is defined by the following equation:

$$C = \frac{\alpha_p{}^{n^*-2}[n^* - 1 - n^*\alpha_p - n^*\alpha_p{}^{n^*-2} + 2n^*\alpha_p{}^{n^*-1} - (n^* - 1)\alpha_p{}^{n^*}]}{(1 - \alpha_p{}^{n^*-1})^2}. \tag{37}$$

The terms in the first braces on the right side of Eq. (36) represent, from left to right respectively: 1) rate of homogeneous nucleation; 2) rate of micelle and monomer droplet nucleation; 3) contribution from the fraction of aqueous phase termination reactions which produces dead polymers with chain length exceeding the critical value n^*; 4) rate of radical capture by particles; 5) rate of aqueous phase termination of radicals; and 6) rate of particle coagulation. α_p, as defined by Eq. (24), is the probability of a radical to add a monomeric unit (i.e., chain propagation). A primary radical needs to add $n^* - 1$ monomeric units before it will reach the critical chain length n^* and precipitate from the aqueous phase as a primary particle. Thus, $\alpha_p{}^{n^*-1}$ in the first term of the first braces on the right side of Eq. (36) is the probability for a primary radical to nucleate a new particle by homogeneous nucleation.

Since $1 - \alpha_p{}^{n^*-1}$ is the probability opposite to that of homogeneous nucleation, the second term in the first braces of Eq. (36) represents the rate of particle formation through micelle and monomer droplet nucleation mechanisms if neither radical capture by particles nor aqueous phase termination occurs in the system. The particle formation rate is reduced by the rate at which the radicals are captured by particles (the 5th term) and the rate of particle coagulation (the 6th term). Since C is always less than unity, the aqueous phase termination of radicals (the 3rd and 4th terms) will further reduce the rate of particle nucleation. Equation (36) also shows that chain transfer in the aqueous phase will decrease the particle nucleation rate since the chain transfer rates ρ_{ia} and ρ_{im} (contained in ρ as defined in Eq. 20) appear in the 4th and 5th negative terms.

The terms within the second braces of Eq. (36) represent the effects of radical desorption from particles. The first term in the second braces shows that desorbed radicals can reinitiate particles and, therefore, increase the particle nucleation rate. The remaining four terms in the second braces of Eq. (36) result from the termination of the desorbed radicals, which may have grown through propagation reactions in the aqueous phase. The positive terms (the 2nd and 3rd terms in the second braces) come from the contribution of those termination reactions which result in dead oligomers with chain length exceeding the critical chain length n^*. In the absence of radical desorption from particles, $K_e = 0$, and all terms in the second braces of Eq. (36) are zero. All these are expected by the mechanism analysis in the previous section.

Equation (36) can be rewritten as

$$(1/N_A)dN/dt = d[\mathrm{P}]/dt = b\rho_i - Bc[\mathrm{P}] - Bf[\mathrm{P}]^2, \tag{38}$$

where

$$b = 1 - (1 - C)k_{tw}B^2 B_i^2 \rho_i, \tag{39}$$

$$Bc = K_c B\rho + 2k_{tw}B\rho\gamma_t - k_p M_w \gamma_a - k_{tw} \sum_{i=1}^{n^*-1} \sum_{j=1}^{i} (\gamma_i \alpha_p{}^{n^*-j} + \gamma_{n^*-j}\alpha_p{}^{i})\, \rho/(k_p M_w), \tag{40}$$

$$Bf = K_f + k_{tw}\gamma_t{}^2 - k_{tw} \sum_{i=1}^{n^*-1} \sum_{j=1}^{i} \gamma_i \gamma_{n^*-j}, \tag{41}$$

$$B_i = \rho/\rho_i = 1 + \rho_{ia}/\rho_i + \rho_{im}/\rho_i. \tag{42}$$

If radical desorption is not significant, Eq. (38) reduces to

$$d[\mathrm{P}]/dt = b\rho_i - K_c B B_i \rho_i [\mathrm{P}] - K_f [\mathrm{P}]^2. \tag{43}$$

Equation (43) is identical in form to that of Eq. (2) which was derived by Fitch and Tsai [6-8] from Priest's [5] homogeneous nucleation mechanism. Equation (43), however, is obtained from detailed modeling of Poehlein's general particle nucleation scheme (Fig. 1) which not only includes homogeneous nucleation but also micelle-entry and monomer-droplet nucleation. It is interesting to note that the derivation of Eq. (2) by Fitch and Tsai need not assume the homogeneous nucleation mechanism. In fact, the form of Eq. (2) can be obtained even if only the micelle entry nucleation mechanism is assumed to be possible in the system. In any case, free radicals generated in the aqueous phase will nucleate particles unless they are all terminated in the aqueous phase. Fitch has introduced the constant b in Eq. (2) to account for the aggregation (i.e., termination) of radicals in the aqueous phase. The parameter b in Eq. (43) is the reciprocal fraction of free radicals generated which terminate in the aqueous phase without producing new particles. Therefore, b should be, and can be shown to be, less than unity.

Please note that the derivation of Eq. (2) by Fitch and Tsai [6-8] does not include the effects of radical desorption and reabsorption on particle nucleation. It is therefore not surprising that their equation becomes a reduced form of our general model (Eq. 38) which includes the contribution from radical desorption and reabsorption. Equation (2) (and also Eq. 43) predicts that the production rate of particles, dN/dt, always decreases with increasing time. On the other hand, Eq. (38) allows the production rate of

particles to increase with time since the contribution from desorbed radicals (represented by the term $k_p M_w \gamma_a$ in Bc of Eq. 40) may cause Bc in Eq. (38) to be negative. Evidence for the production rate of particles increasing with time has been reported by Lichti et al. [33] and Feeney et al. [34, 35]. They observed that the curves of particle size distribution (PSD) obtained just before the end of Interval I always skewed toward small particle size. They showed that this phenomenon could only be explained by an increasing rate of production of new latex particles.

SOLUTION FOR TOTAL PARTICLE NUMBER

Equation (38) can be solved to predict the particle concentration in the transient state. Before doing so, an analysis of the parameters in the equation is helpful. For a given system, M_w can be considered the monomer solubility in water and therefore is treated as a constant. In principle, K_e, K_c and K_f are particle-size dependent and should be time dependent. However, during Interval I of particle nucleation, change of particle size with time is small so that these parameters can be considered to be time independent. With this argument, the parameter $\gamma = K_e/(k_p M_w)$ in Eq. (25) is constant. Since $[M_i]$, $[M_{i-1}]$ and $[Pm_i]$ are constant because of the radical steady state (Assumption 4), Eq. (27) shows that α_p must also be constant. If we also assume ρ_i, ρ_{im}, and ρ_{ia} change little during Interval I, b (Eq. 39), Bc (Eq. 40), and Bf (Eq. 41) in Eq. (38) can be taken as time independent. Thus, the only time-dependent variable in Eq. (38) is the particle concentration [P]. Integrating Eq. (38) with initial condition, $[P] = Q_0$ at $t = 0$, yields

$$[P] = \frac{Q_1 - \beta Q_2}{1 + \beta}, \tag{44}$$

$$\beta = \frac{Q_1 - Q_0}{Q_2 + Q_0} e^{-K_f(Q_1 + Q_2)t} \tag{45}$$

where

$$Q_1 = \frac{\sqrt{Bc^2 + 4b\rho_i Bf} - Bc}{2Bf}, \tag{46}$$

$$Q_2 = \frac{\sqrt{Bc^2 + 4b\rho_i Bf} + Bc}{2Bf}. \tag{47}$$

Q_0 is the concentration of seed particles which exist at tht beginning of the polymerization. Equations (44) and (45) show that [P] approaches Q_1 when t becomes large. Thus, Q_1 can be considered the particle concentration at steady state. In fact, the same expression as Eq. (46) can be obtained by setting $d[\mathrm{P}]/dt = 0$ and solving Eq. (38) for the steady-state particle concentration $[\mathrm{P}]_s$. As a consequence, Eqs. (44) and (45) can be rearranged to give a dimensionless form of particle concentration.

$$\frac{N}{N_s} = \frac{[\mathrm{P}]}{[\mathrm{P}]_s} = \frac{1 - A_2\beta'}{1 + \beta'}, \tag{48}$$

$$\beta' = \frac{1 - A_1}{A_1 + A_2} e^{-(t/\tau)}, \tag{49}$$

where

$$A_1 = Q_0/[\mathrm{P}]_s = Q_0/Q_1, \tag{50}$$

$$A_2 = Q_2/Q_1, \tag{51}$$

$$\tau = \frac{1}{BfQ_1(1 + A_2)}. \tag{52}$$

Results computed from Eq. (48) are shown in Figs. 2 through 5. Figure 2 shows variation of polymer particle number with time for the systems in which no particles exist at the beginning (i.e., $A_1 = 0$). The particle number N increases with time until it finally reaches a steady state ($N/N_s = 1$). τ is a parameter with the dimension of time. The smaller the value of τ, the more rapidly the particle number N will reach its steady state. A_2 is another parameter which can change the shape of the N vs t curves. When $A_2 > 1.0$, N/N_s increases rapidly at the beginning and then more slowly. If $A_2 < 1.0$, the N/N_s vs t/τ curve becomes sigmoidal. The influence of parameters A_2 and τ on the rate of change of N with time can be best demonstrated by Fig. 3, in which $d(N/N_s)/d(t/\tau)$ is plotted against dimensionless time (t/τ). When $A_2 > 1.0$, $d(N/N_s)/d(t/\tau)$ is a monotonically decreasing function of t/τ. This kind of dN/dt vs t curves has been predicted by the Smith-Ewart model [4], the Fitch-Tsai model [7], and the Hansen-Ugelstad model [9]. When A_2 is less than 1.0, $d(N/N_s)/d(t/\tau)$ increases first, passes a maximum, and then decreases. The two-step coagulation model proposed by Lichti et al. [33] and Feeney et

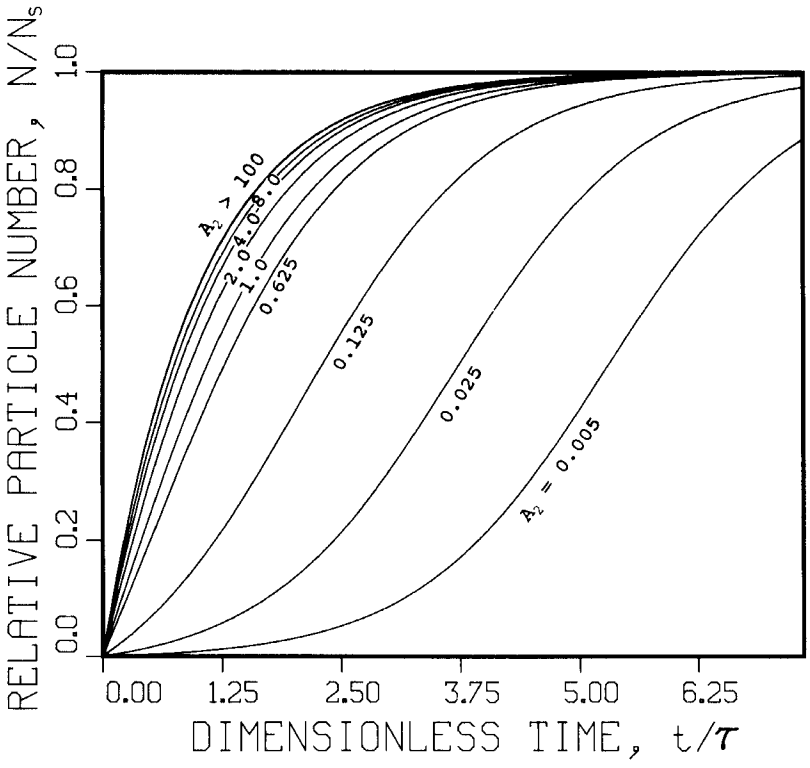

FIG. 2. Transient particle number profiles.

al. [34] also predicts this type of dN/dt vs t curve. Thus, our model has been able to simulate all types of dN/dt vs t curves reported in the literature. Figure 2 can be used when τ, A_2, and N_s can be determined from known recipe ingredients and reacter parameters for a particular system computed from Eqs. (24), (35), (39)-(42), (46), (47), (51), and (52).

The variation of polymer particle concentration with time for seeded emulsion polymerization systems ($A_1 > 0$) is shown in Figs. 4 and 5 for $A_2 = 5$ and 0.025, respectively. When A_1 is less than 1.0, N increases with time to approach the steady-state value N_s, while for the systems with A_1 greater than unity, N decreases with time to approach N_s. This demonstrates that when N_0 is greater than N_s, coagulation of particles proceeds faster than particle generation. Most radicals are captured by seed particles, and some coagulation

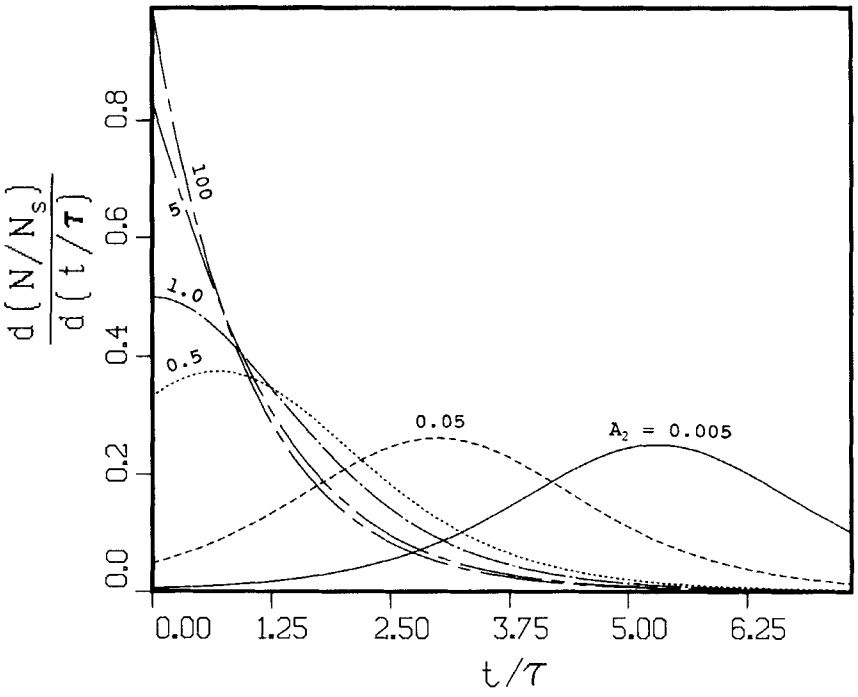

FIG. 3. Influence of parameters A_2 and τ on the rate of particle formation.

occurs. Although it is difficult to obtain a stable seed latex with a particle number that exceeds the steady-state value, situations in which the particle number exceeds the steady-state particle number indeed occur during the emulsion polymerization of some systems. An examination of the *N-t* curves of Fitch and Tsai [7] and Dunn and Chong [40] shows that particle numbers for emulsifier-free systems increase rapidly at the beginning of the reaction, pass a maximum, and then decrease with time to tend toward the steady-state value. The decreasing part of the *N-t* curves can then be simulated with the present model by using values for parameter A_1 greater than unity. The rapid increase in particle number during early stages of particle nucleation can be attributed to the small particle size, which reduces the ability of particles to capture free radicals in the aqueous phase and a rapid decrease in n^*. This phenomenon is examined in another paper [42]. The theory developed in this paper is based on constant n^*. Therefore, the model results

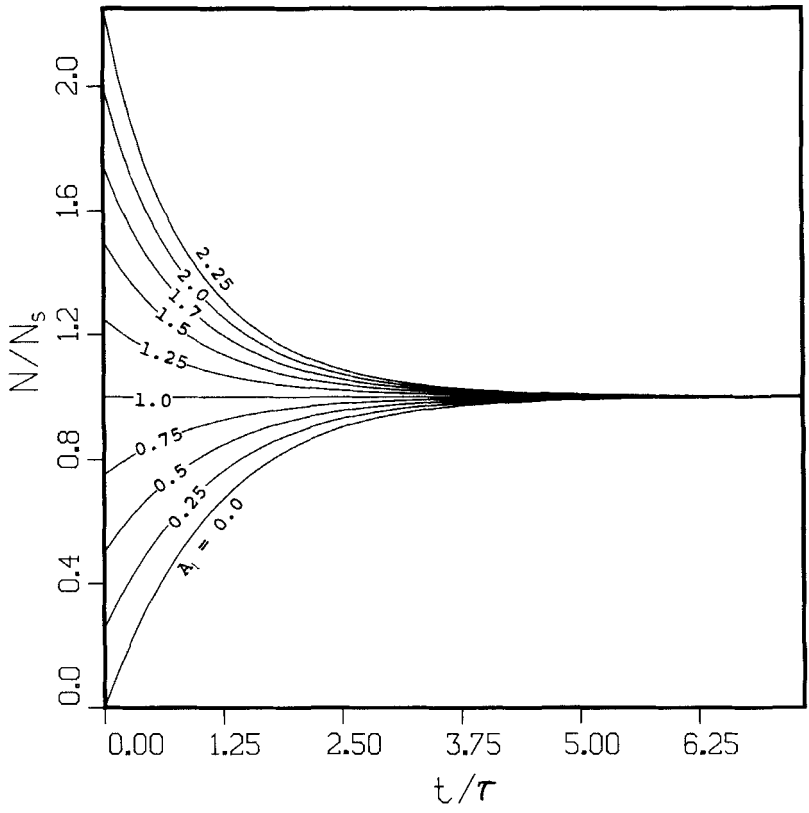

FIG. 4. Transient particle number profiles for seeded systems ($A_2 = 5$).

are only applicable to the decreasing part of the N-t curves of emulsifier-free systems, where n^* has reached its steady-state value.

Since τ is an important parameter in the model and has the dimension of time, its physical meaning is important. The definition of τ (Eq. 52) shows that its dimension comes from the term $1/(Bf[\mathrm{P}]_s)$. The aqueous-phase termination of desorbed radicals is neglected, thus, $Bf = K_f$. The rate of particle coagulation is equal to $K_f[\mathrm{P}]_s^2$ at the steady state. $\tau_s = 1/(K_f[\mathrm{P}]_s)$ is then the time needed for $[\mathrm{P}]_s$ particles to disappear by coagulation. Another way to interpret the meaning of τ_s is to imagine a system which has reached its steady-state particle concentration $[\mathrm{P}]_s$ which then coagulates at the rate $K_f[\mathrm{P}]_s^2$.

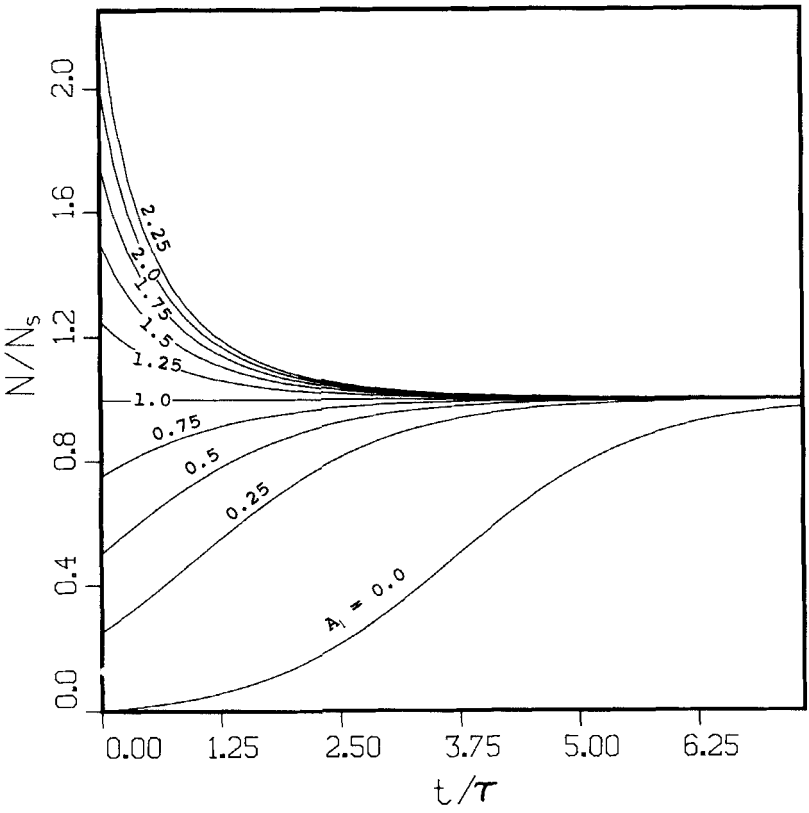

FIG. 5. Transient particle number profiles for seeded systems (A_2 = 0.025).

The number of newly formed particles per unit volume per unit time is equal to $K_f[P]_s^2$. Because $K_f[P]_s^2$ is much smaller than $[P]_s$, it will not affect the coagulation rate at the steady state. Thus, τ_s can also be considered to be the time during which $[P]_s$ particles would be produced per unit volume at the steady state if no particle coagulation were occurring in the system. Therefore, the smaller τ_s, the faster the particle concentration will increase to reach its steady-state value $[P]_s$. The model parameter τ in Eq. (52) has the same physical meaning as that of τ_s with regard to the time to reach the steady state of particle concentration, except that τ contains another dimensionless model parameter A_2 which tends to increase the influence of τ_s.

ESTIMATION OF THE MODEL PARAMETERS

Use of the model developed in the last section requires estimation of the model parameters A_2, τ, and Q_1. These parameters are all function of the propagation probability α_p which can be estimated in the following way.

When desorption of free radicals from particles can be neglected (i.e., $\gamma = 0$), the following equation is obtained by substituting Eqs. (12), (31), and (32) into Eq. (10) with the assumption of steady-state concentration of free radicals.

$$\rho_i - \alpha_p{}^{n^*-1}\rho - \frac{K_{mc}[\mathrm{Mc}] + K_{md}[\mathrm{Md}] + K_c[\mathrm{P}]\,\rho\alpha_p(1 - \alpha_p{}^{n^*-1})}{k_p \mathrm{M}_w(1 - \alpha_p)}$$

$$- \frac{k_{tw}}{k_p{}^2 \mathrm{M}_w{}^2}\,\rho^2\alpha_p{}^2\left(\frac{1 - \alpha_p{}^{n^*-1}}{1 - \alpha_p}\right)^2 = 0. \tag{53}$$

Rearranging the above equation yields

$$D_1(1 - \alpha_p{}^{n^*-1})[\alpha_p/(1 - \alpha_p)]^2 + D_2[\alpha_p/(1 - \alpha_p)] - 1 = D_3(1 - \alpha_p{}^{n^*-1}), \tag{54}$$

where

$$D_1 = \frac{k_{tw}\rho}{(k_p \mathrm{M}_w)^2}, \tag{55}$$

$$D_2 = \frac{K_{mc}[\mathrm{Mc}] + K_{md}[\mathrm{Md}] + K_c[\mathrm{P}]}{k_p \mathrm{M}_w}, \tag{56}$$

$$D_3 = \frac{\rho - \rho_i}{\rho}. \tag{57}$$

Equations (54) and (32) can then be solved simultaneously to obtain α_p and $[\mathrm{R}_w]$ using a proper iteration procedure. First, an initial value of α_p is assumed to calculate $[\mathrm{R}_w]$ from Eq. (32). The calculated $[\mathrm{R}_w]$ is then used in estimating D_1 and D_3 with Eqs. (55) and (57). If D_2 is also estimated, a new value of α_p can be obtained by solving Eq. (54). This value of α_p is then compared with the assumed α_p value. If the difference exceeds the required error limit, the new α_p value is then used in Eq. (32) to estimate another $[\mathrm{R}_w]$ value. The iteration procedure continues until the required error limit is satisfied.

When chain transfer reactions can be neglected (i.e., $\rho = \rho_i$, $D_3 = 0$), Eq. (54) reduces to

$$D_1(1 - \alpha_p{}^{n^*-1})[\alpha_p/(1 - \alpha_p)]^2 + D_2[\alpha_p/(1 - \alpha_p)] - 1 = 0. \tag{58}$$

Equation (58) is readily solved for α_p using a Newtonian iteration method. The initial value for iteration can be estimated from the following equation, which is obtained from Eq. (58) assuming $\alpha_p{}^{n^*-1} << 1$:

$$\alpha_p = \frac{\sqrt{D_2{}^2 + 4D_1} - D_2}{\sqrt{D_2{}^2 + 4D_1} - D_2 + 2D_1} \tag{59}$$

The initiation rate ρ_i needed in estimating D_1 can be determined by

$$\rho_i = 2fk_d[\mathrm{I}], \tag{60}$$

where [I] is initiator concentration, k_d is the decomposition rate constant of the initiator, and f is the initiation efficiency.

D_2 is assumed to be constant in the model simulation since micelles and monomer droplets are transformed into particles. The increase in the particle concentration [P] counterbalances the decreases in micelle and monomer droplet concentrations, [Mc] and [Md], in Eq. (56), thus maintaining D_2 approximately constant. D_2 is estimated by the following equation for systems in which micelle nucleation mechanism is dominant.

$$D_2 = \delta_m K_{mc}[\mathrm{Mc}]_0/(k_p \mathrm{M}_w), \tag{61}$$

where $[\mathrm{Mc}]_0$ is the initial concentration of micelles and δ_m is the parameter introduced to take into account the difference between K_{mc} and K_c and also the disappearance of micelles needed to adsorb on the particle surface produced through particle growth by polymerization. The initial micelle concentration $[\mathrm{Mc}]_0$ is related to the emulsifier concentration charged [S] by

$$[\mathrm{Mc}]_0 = ([\mathrm{S}] - \mathrm{CMC})/j_m, \tag{62}$$

where CMC is the critical micelle concentration of the emulsifier used and j_m is the number of emulsifier molecules comprising a micelle.

The rate coefficients for free radical capture by particles and micelles, K_c and K_{mc}, respectively, can be estimated assuming a diffusion model as proposed by Hansen and Ugelstad [9]. Thus

$$K_c = 4\pi r_p D_w N_A, \tag{63}$$

$$K_{mc} = 4\pi r_m D_w N_A, \tag{64}$$

where N_A is Avogadro's number, D_w is the diffusion coefficient of free radicals in the aqueous phase, and r_p and r_m are the average radii of the particles and micelles, respectively.

Once the propagation probability in the aqueous phase, α_p, is determined, the model parameters Q_1, A_2, and τ can be estimated by Eqs. (46), (47), (51), and (52) from the known kinetic parameters and the reaction conditions.

EXPERIMENTAL TEST OF THE MODEL

The experimental data of Chatterjee [23] and Zollars [28] are listed in Tables 1 and 2. Recipes and reaction conditions of the experiments are also listed in the tables. Particle number data presented in Zollars' paper were measured by light-scattering techniques and, therefore, are weight averages, while the kinetic expressions require a number average, Zollars [28] pointed out that Vanso [43] and Friis and Nyhagen [44] had determined that the number-average particle number should be 2.6 times greater than the weight-average for vinyl acetate emulsion polymerization. This 2.6 factor has been used to convert Zollars' original data to those presented in Table 2.

The kinetic parameters used in model simulations are listed in the upper part of Table 3. Values of 2.86×10^{-10} dm^2/s for D_w, 2.1 nm for the micelle radius r_m, and 60 for j_m are assumed in the model simulation for all experimental conditions. Hansen and Ugelstad [9] used 10^{-8} and 10^{-10} for D_w in their model simulation, but they suggested that the value of 10^{-10} was more realistic. Odian [46] reported that a micelle is comprised of 50 to 150 emulsifier molecules with a diameter of 2 to 10 nm.

The particle number N was calculated with the values listed in the upper part of Table 3, along with an appropriate choice of values for the initiator efficiency f, average coagulation rate coefficient K_f, and the parameter δ_m. The results are compared with the experimental data as shown in Figs. 6 and 7. The squares in the figures are experimental data. The solid lines are the model predictions. The good agreement between experiment and theory is evident. The values of f, K_f, and δ_m chosen and the model parameters A_2, τ, and N_s of Eq. (48) calculated for the different experimental systems are all listed in the lower part of Table 3.

TABLE 1. Chatterjee's Data[a] [23]

t, min	10.0	14.0	19.0	22.0	27.6	32.5	49.0	62.6
x,[b] %	8.5	16.5	23.0	23.0	38.8	47.5	70.0	81.0
N, 10^{15} 1/mL	1.69	2.10	2.46	2.79	2.81	2.84	2.92	2.76

[a]Recipe: styrene (5 vol%), water (59 vol%), $K_2S_2O_8$ (0.1%) soap (0.6%) at 50°C.

[b]x = monomer conversion.

The values of 0.925 for f and 250 L/(mol·s) for K_f give the best fit for the experimental data of styrene by Chatterjee [23] (Fig. 6), while values of 0.142 for f and 130 L/mol·s for K_f gives the best fit for the experimental data of vinyl acetate by Zollars [28] (Fig. 7). It is not unreasonable that different systems would have different values of f and K_f. Fitch and Tsai [7] have chosen f values of 0.09, 0.1, and 1.0 to fit their model to the experimental methyl methacrylate data using different initiators and different emulsifier concentrations. The value of K_f for the Chatterjee system is greater than that for the Zollars system. This may be attributed to the difference in particle size between the two systems. The particle size of the Chatterjee system (r_p = 14 nm) is smaller than that of the Zollars system (r_p = 35 nm). As discussed previously, small particles have a stronger tendency to coagulate than large particles. Therefore, the Chatterjee system has a greater value for the coagulation rate coefficient.

TABLE 2. Zollars' Data[a] [28]

t, min	90	120	150	180	210
x,[b] %	41	55	72	82	90
N, 10^{14} 1/mL	3.43	3.64	4.39	4.78	5.15

[a]Recipe: vinyl acetate (614 g), water (1817 g), $K_2S_2O_8$ (0.125×10^{-3} M), sodium cetyl sulfate (10.9 g) at 60°C.

[b]x = monomer conversion.

TABLE 3. Kinetic Data Used in Calculation and the Model Parameters Calculated[a]

System	Chatterjee	Zollars	Refs.
Monomer	St	VA	
M_w, mol/L	0.0035	0.29	41
CMC, mol/L	0.009	0.0062	45
[S], mol/L	0.0208	0.02	Tables 1 and 2
[I] $\times 10^3$, mol/L	3.699	0.125	Tables 1 and 2
$r_p \times 10^7$, dm	1.40	3.5	23, 28
$r_m \times 10^8$, dm	2.1	2.1	46
Temperature, °C	50	60	Tables 1 and 2
$k_d \times 10^6$, 1/s	0.95	3.16	45
k_p, L/(mol·s)	209	12000	45
$k_{tw} \times 10^{-8}$, L/(mol·s)	1.15	4.81	45
$C_m \times 10^4$	0.5	2.0	45
n^*	5	85[b]	47
$D_w \times 10^{10}$, dm^2/s	2.86	2.86	9
f	0.925	0.142	
δ_m	1.0	1.0	
K_f, L/(mol·s)	250	130	
$N_s \times 10^{-16}$, 1/L	282	20.7	
A_2	1.188	1.032	
τ, min	6.513	69.49	

[a] C_m = chain transfer constant for monomer.
[b] Assumed

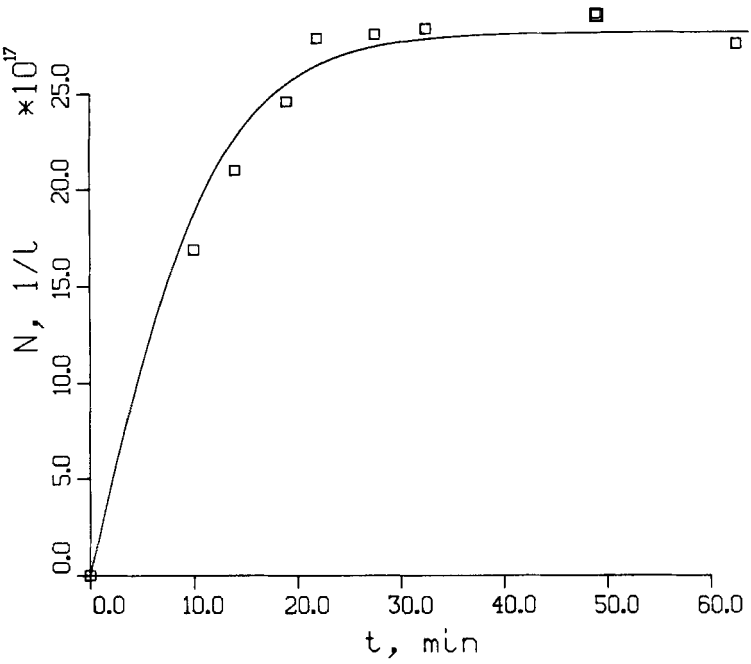

FIG. 6. Comparison of the model prediction (solid line) with the experimental data (marks) of styrene by Chatterjee [23]. The solid line is calculated using $\delta_m = 1.0$, $f = 0.925$, and $K_f = 250$ L/mol·s. The model parameters of Eq. (48) calculated from these values are $A_2 = 1.188$, $\tau = 6.513$ min, and $N_s = 2.818 \times 10^{18}$ 1/L.

Hansen and Ugelstad [11] developed an equation based on diffusion theory to calculate the coagulation rate constant $K_{f_{pq}}$ between particles of size p and size q:

$$K_f = \frac{2kT}{3\eta W_{pq}}(p^{1/3} + q^{1/3})(p^{-1/3} + q^{-1/3}), \tag{65}$$

where k is Bolzmann's constant (1.38×10^{-23} J/K), T is absolute temperature, η is the viscosity of the medium, W_{pq} is the Fuchs' stability ratio [48], a function of p and q. The radius of particles with size p, r_p, is related to the radius of the primary particles, r_1, by

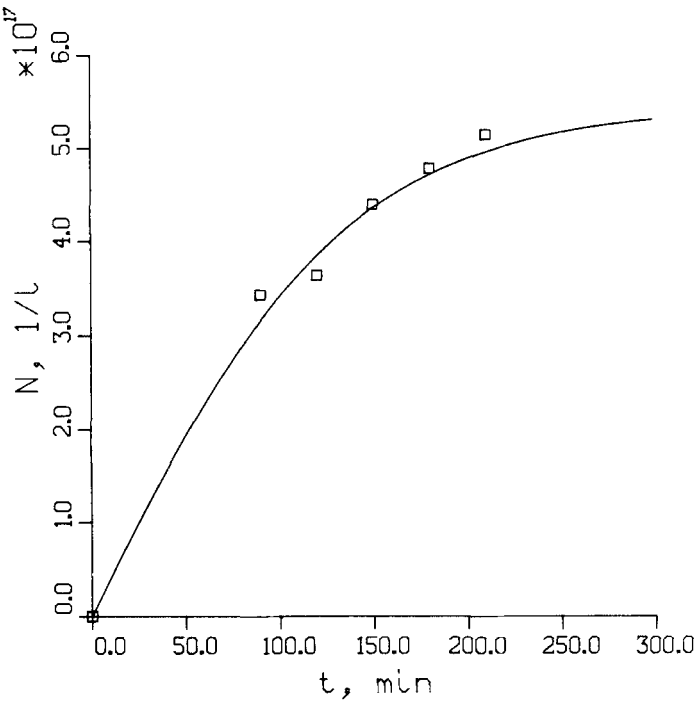

FIG. 7. Comparison of the model prediction (solid line) with the experimental data (marks) of vinyl acetate by Zollars [28]. The solid line is calculated using $\delta_m = 1.0$, $f = 0.142$, and $K_f = 130$ L/mol·s. The model parameters of Eq. (48) calculated from these values are $A_2 = 1.032$, $\tau = 69.49$ min, and $N_s = 2.07 \times 10^{17}$ 1/L.

$$r_p = r_1 p^{1/3}. \tag{66}$$

If we consider the coagulation between particles of equal size p, Eq. (65) is reduced to

$$K_f = \frac{8kT}{3\eta W_{pq}}, \tag{67}$$

where W_{pq} can be found from Fig. 8 as a function of p for $r_1 = 2$ nm. Chatterjee's experimental data for styrene (Table 1), were obtained at $T = 323$ K.

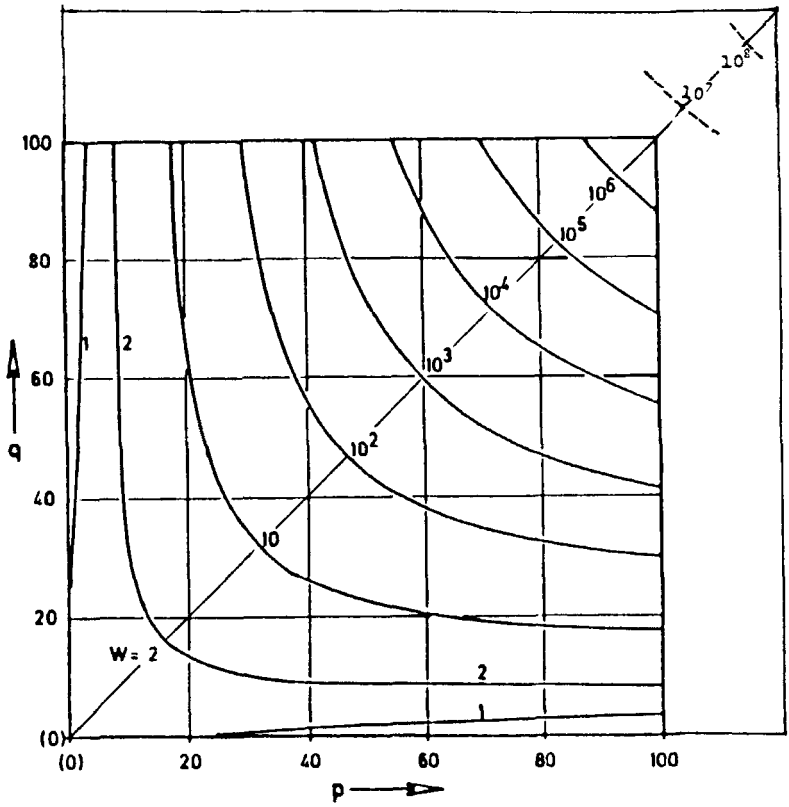

FIG. 8. Contour map of Fuchs' stability ratio W_{pq} as a function of class indices p and q. $T = 60°C$. Hansen and Ugelstad [9].

The parameter K_f has been determined to be 250 L/(mol·s) by fitting our model of the particle concentration to the experimental data in Table 1. Substituting this value of K_f and $\eta = 0.5494$ cP into Eq. (67), the Fuchs' stability ratio, W_{pp}, is calculated to be 5.212×10^7. This value is beyond the range of Fig. 8, since the largest W_{pp} shown by Hansen and Ugelstad's graph [9] is about 8×10^6 which corresponds to $p = 100$. By extrapolating (Fig. 8), we obtain $p = 110$ for $W_{pp} = 5.212 \times 10^7$. Thus, the particle diameter can be calculated from Eq. (66) for $r_1 = 2$ nm to be about 19.1 nm. Similarly, the particle diameter obtained in this manner for Zollars' experimental data with vinyl acetate (Table 2) is 19.6 nm, using $K_f = 130$ L/(mol·s), $T = 333$ K,

and $\eta = 0.4888$ cP. The diameter so obtained may be called the coagulation-average diameter and is defined as

$$d_f^2 = \frac{\sum_{i=1}^{\infty}\sum_{j=1}^{\infty} K_{f_{ij}} d_i d_j}{\sum_{i=1}^{\infty}\sum_{j=1}^{\infty} k_{f_{ij}}}, \tag{68}$$

where d_i is the diameter of particles of size i. The measured particle diameters estimated at about 40% conversion are about 28 and 70 nm (Table 3) for Chatterjee's system and Zollars' system, respectively. Thus, the coagulation-average diameters ($d_f = 19.1$ and 19.6 nm for Chatterjee's system and Zollars' system, respectively) are much less than the measured particle diameters. This is not surprising since, as indicated before, small particles have a much stronger tendency to coagulate. The value of K_f determined in the manner described in this paper is weighted toward small particles. The d_f determined from K_f, therefore, reflects mainly the diameter of these small particles.

SUMMARY

A general kinetics model of particle formation in emulsion polymerization has been developed. This model takes into account homogeneous, micelle, and monomer droplet nucleation mechanisms. Chain transfer and termination in the aqueous phase, capture of oligomer radicals by particles, and coagulation of particles are also included in the model. An analytical solution (Eq. 48) is obtained for the transient particle concentration. Variation of particle concentration as well as particle generation rate with time (Figs. 2 and 3, respectively) for different values of the model parameters are presented. When $A_2 > 1.0$, the production rate of particles always decreases with time (Fig. 3). When $A_2 < 1.0$, the production rate of particles increases with time first, passes a maximum, and then decreases (Fig. 3), while the N vs t curves present a sigmoidal shape (Fig. 2). This model of transient particle concentration fits the experimental data of the emulsion polymerization of the styrene and vinyl acetate systems. The values of the average coagulation rate coefficient K_f obtained from the fitting procedure were used to determine the coagulation-average particle diameter. The fact that the coagulation-average particle diameter calculated is much less than the observed number-average particle diameter con-

firms that small particles have a much stronger tendency to coagulate than large particles.

APPENDIX

Derivation of Eqs. (36) and (37)

Substituting Eqs. (31) and (32) into Eq. (3) gives

$$\frac{d[\mathrm{P}]}{dt} = k_p \mathrm{M}_w \left\{ \frac{\rho \alpha_p{}^{n^*-1}}{(k_p \mathrm{M}_w)} + \gamma_{n^*-1}[\mathrm{P}] \right\} + (K_{mc}[\mathrm{Mc}] + K_{md}[\mathrm{Md}])(B\rho + \gamma_t[\mathrm{P}]) - K_f[\mathrm{P}]^2 + k_{tw} \sum_{i=1}^{n^*-1} \sum_{j=1}^{i} \left\{ \frac{\alpha_p{}^i \rho}{(k_p \mathrm{M}_w)} + \rho_i[\mathrm{P}] \right\} \left\{ \frac{\alpha_p{}^{n^*-1}}{(k_p \mathrm{M}_w)} + \gamma_{n^*-j}[\mathrm{P}] \right\} = \left\{ \rho \alpha_p{}^{n^*-1} + k_p \mathrm{M}_w \gamma_{n^*-1}[\mathrm{P}] \right\} + \left\{ [(1-\alpha_p)/\alpha_p] k_p \mathrm{M}_w [\mathrm{R}_w] - K_c[\mathrm{P}][\mathrm{R}_w] - k_{trm}[\mathrm{R}_w]\mathrm{M}_w - k_{tr}[\mathrm{CTA}]_w[\mathrm{R}_w] - k_{tw}[\mathrm{R}_w]^2 \right\} - K_f[\mathrm{P}]^2 + k_{tw} \sum_{i=1}^{n^*-1} \sum_{j=1}^{i} \left\{ \frac{\alpha_p{}^i \rho}{(k_p \mathrm{M}_w)} + \gamma_i[\mathrm{P}] \right\} \left\{ \frac{\alpha_p{}^{n^*-i}}{(k_p \mathrm{M}_w)} + \gamma_{n^*-j}[\mathrm{P}] \right\}$$

$$= \rho_i \alpha_p{}^{n^*-1} + \rho_i(1 - \alpha_p{}^{n^*-1}) + k_p \mathrm{M}_w \gamma_a[\mathrm{P}] - K_c[\mathrm{P}][\mathrm{R}_w] - k_{tw}[\mathrm{R}_w]^2 - K_f[\mathrm{P}]^2 + k_{tw} \sum_{i=1}^{n^*-1} \sum_{j=1}^{i} \left\{ \frac{\alpha_p{}^i \rho}{k_p \mathrm{M}_w} + \gamma_i[\mathrm{P}] \right\} \left\{ \frac{\alpha_p{}^{n^*-j} \rho}{k_p \mathrm{M}_w} + \gamma_{n^*-j}[\mathrm{P}] \right\} = \rho_i \alpha_p{}^{n^*-1} + (1 - \alpha_p{}^{n^*-1}) + k_p \mathrm{M}_w \gamma_{n^*-1}[\mathrm{P}] - K_c[\mathrm{P}](B\rho + \gamma_t[\mathrm{P}]) - k_{tw}(B\rho + \gamma_t[\mathrm{P}])^2 - K_f[\mathrm{P}]^2 + k_{tw} \sum_{i=1}^{n^*-1} \sum_{j=1}^{i} \left\{ \frac{\alpha_p{}^i \rho}{k_p \mathrm{M}_w} + \gamma_t[\mathrm{P}] \right\} \left\{ \frac{\alpha_p{}^{n^*-j} \rho}{k_p \mathrm{M}_w} + \gamma_{n^*-j}[\mathrm{P}] \right\}, \quad \text{(A1)}$$

where

$$\gamma_a = k_p \mathrm{M}_w [\mathrm{P}] \left\{ \gamma_{n^*-1} + \gamma_t(1 - \alpha_p)/\alpha_p \right\}. \quad \text{(A2)}$$

Rearranging Eq. (A1) gives Eq. (36).

The third term in the first brace of Eq. (36) is derived from Eq. (A1).

$$k_{tw}B^2\rho^2C = K_{tw}\sum_{i=1}^{n^*-1}\sum_{j=1}^{i}\frac{\rho^2\alpha_p{}^i\alpha_p{}^{n^*-j}}{(k_p\mathrm{M}_w)^2} = \frac{k_{tw}\rho^2}{(k_p\mathrm{M}_w)^2}\,\alpha_p{}^{n^*}\sum_{i=1}^{n^*-1}\sum_{j=1}^{i}\alpha_p{}^{i-j}. \tag{A3}$$

Therefore

$$\begin{aligned}\sum_{i=1}^{n^*-1}\sum_{j=1}^{i}\alpha_p{}^{i-j} &= \left\{(n^*-1)+(n^*-2)\alpha_p+(n^*-3)\alpha_p{}^2+\cdots+\alpha_p{}^{n^*-2}\right\}\\ &= \sum_{j=1}^{n^*-1}(n^*-j)\alpha_p{}^{j-1}\\ &= \sum_{j=1}^{n^*-1}n^*\alpha_p{}^{j-1}-\sum_{j=1}^{n^*-1}j\alpha_p{}^{j-1}\\ &= n^*\frac{1-\alpha_p{}^{n^*-2}}{1-\alpha_p}-\sum_{j=1}^{n^*-1}j\alpha_p{}^{j-1}. \end{aligned}\tag{A4}$$

Therefore

$$\begin{aligned}\sum_{j=1}^{n^*-1}j\alpha_p{}^{j-1} &= \frac{d}{d\alpha_p}\left(\sum_{j=1}^{n^*-1}\alpha_p{}^j\right) = \frac{d}{d\alpha_p}\left\{\frac{\alpha_p(1-\alpha_p{}^{n^*-1})}{1-\alpha_p}\right\}\\ &= \left\{1-n^*\alpha_p{}^{n^*-1}+(n^*-1)\alpha_p{}^{n^*}\right\}/(1-\alpha_p)^2.\end{aligned}$$

Substituting the above equation into Eq. (A4) yields

$$\begin{aligned}&\sum_{i=1}^{n^*-1}\sum_{j=1}^{i}\alpha_p{}^{i-j}\\ &= \frac{\left\{(n^*-1)-n^*\alpha_p-n^*\alpha_p{}^{n^*-2}+2n^*\alpha_p{}^{n^*-1}-(n^*-1)\alpha_p{}^{n^*}\right\}}{(1-\alpha_p)^2}\\ &= \frac{\alpha_p{}^2(1-\alpha_p{}^{n^*-1})^2}{(1-\alpha_p)^2}\,\frac{(n^*-1)(1-\alpha_p{}^{n^*})+n^*(2\alpha_p{}^{n^*-1}-\alpha_p{}^{n^*-2}-\alpha_p)}{\alpha_p{}^2(1-\alpha_p{}^{n^*-1})^2}\end{aligned}$$

$$= (k_p M_w)^2 B^2 \frac{(n^* - 1)(1 - \alpha_p{}^{n^*}) + n^*(2\alpha_p{}^{n^*-1} - \alpha_p{}^{n^*-2} - \alpha_p)}{\alpha_p{}^2(1 - \alpha_p{}^{n^*-1})^2}. \quad \text{(A5)}$$

Equation (37) for C is obtained by substituting Eq. (A5) into the right side of Eq. (A3).

SYMBOLS

$A^\cdot$	chain transfer agent radical
CTA	chain transfer agent which represents any possible chain transfer species in the aqueous phase other than monomer
f	initiation efficiency
I	initiator
K_{mc}	rate constant of micelle entry nucleation, L/(mol·s) (K_{mc}' for absorption; K_{mc}'' for desorption).
K_c	rate constant of radical capture by particles (Kc_j, capture constant by P_j particles), L/(mol·s)
k_d	rate constant of initiator decomposition, 1/s
K_e	rate constant of radical escaping from particles (Ke_j, for escape of radicals with chain length i), L/(mol·s)
K_f	rate constant of particle coagulation ($K_{f_{ij}}$, coagulation between P_i particles and P_j particles), L/(mol·s)
k_i	rate constant of initiation from initiator radicals
k_{ia}	rate constant of initiation from $A^\cdot$ radicals
k_{ic}	rate constant of capture of $R^\cdot$ or $A^\cdot$ radicals by micelles, L/(mol·s) (k_{ic}' for absorption, k_{ic}'' for desorption)
k_{id}	rate constant of absorption of $R^\cdot$ or $A^\cdot$ radicals by monomer deoplets, L/(mol·s) (k_{id}' for absorption, k_{id}'' for desorption)
K_{md}	rate constant of monomer droplet entry nucleation (K_{md}' for absorption; K_{md}'' for desorption), L/(mol·s)
k_p	propagation rate constant in the aqueous phase, L/(mol·s)
k_{ta}	rate constant of termination between oligomeric radicals and CTA radicals $A^\cdot$, L/(mol·s)

k_{ti} rate constant of termination between oligomeric radicals and initiator radicals, L/(mol·s)

k_{tr} rate constant of chain transfer to CTA, L/(mol·s)

k_{trm} rate constant of chain transfer to monomer, L/(mol·s)

k_{tw} termination rate constant in the aqueous phase, L/(mol·s)

M monomer in the aqueous phase

$\bar{m}_i$ average number of radicals with chain length i per particle

Mc micelle

Md monomer droplet

M_i oligomeric radical with chain length i

M_w monomer concentration in the aqueous phase, mol/L

N particle number concentration, particles/(L·w)

$\bar{n}$ average radical number per particle, $\bar{n} = \sum_{i=1}^{\infty} \bar{m}_i$

n^* critical chain length

O_i dead oligomer with chain length i

P polymer particles

Pa particles formed from homogeneous nucleation

Pc particles formed from micelle entry nucleation

Pd particles formed from monomer droplet nucleation

P_i particles which have been initiated i times ($P_i = Pa_i + Pb_i + Pd_i$, $i = 1, 2, \ldots$)

$[Pm_i]$ concentration of radicals with chain length i in the particle phase

$R^{\bullet}$ primary radicals from initiator

R_{mb} rate of micelle disappearance to cover newly formed particle surface

R_{md}' rate of monomer droplet coalescence

R_{md}'' rate of monomer droplet separation

R_{tw} aqueous phase termination rate, mol/(L·s)

$[R_w]$ total concentration of oligomeric radicals in the aqueous phase, mol/L·s

ρ_i initiation rate, mol/L·s

REFERENCES

[1] W. D. Harkins, *J. Am. Chem. Soc., 69,* 1428 (1947).
[2] W. D. Harkins, *J. Polym. Sci., 5,* 217 (1950).
[3] W. V. Smith and R. W. Ewart, *J. Chem. Phys., 16,* 592 (1948).
[4] W. V. Smith, *J. Am. Chem. Soc., 70,* 3695 (1948).
[5] W. J. Priest, *J. Phys. Chem., 56,* 1077 (1952).
[6] R. M. Fitch and C. H. Tsai, *J. Polym. Sci., Part B, Polym. Lett., 8,* 703 (1970).
[7] R. M. Fitch and C. H. Tsai, in *Polymer Colloids* (R. M. Fitch, ed.), Plenum, New York, 1971.
[8] R. M. Fitch, in *Emulsion Polymers and Emulsion Polymerization* (D. R. Bassett and A. E. Hamelec, eds.), (ACS Symp. Ser. 165), Washington, D.C., 1981.
[9] F. K. Hansen and J. Ugelstad, *J. Polym. Sci., Polym. Chem. Ed., 16,* 1953 (1978).
[10] F. K. Hansen and J. Ugelstad, *Ibid., 17,* 3033 (1979).
[11] F. K. Hansen and J. Ugelstad, *Ibid., 17,* 3047 (1979).
[12] F. K. Hansen and J. Ugelstad, *Ibid., 17,* 3068 (1979).
[13] V. Kamath, PhD Thesis, University of Akron, Akron, Ohio, 1973.
[14] I. Piirma, in *Emulsion Polymerization* (I. Piirma, ed.), (ACS Symp. Ser. 24), Washington, D.C., 1976.
[15] C. P. Roe, *Ind. Eng. Chem., 60*(9), 20 (1968).
[16] T. Nakagawa and H. Inoue, *Nippon Kagaku Zasshi, 78,* 636 (1957).
[17] K. Kuryana, H. Inoue, and T. Nakagawa, *Kolloid Z. Z. Polym., 183*(1), 68 (1962).
[18] M. E. Wood, J. S. Dodge, J. M. Krieger, and P. E. Piece, *J. Paint Technol., 40*(57), 543 (1968).
[19] A. S. Dunn and W. A. Al-Shahib, *Br. Polym. J., 10,* 137 (1978).
[20] A. S. Dunn and W. A. Al-Shahib, in *Polymer Colloids II* (R. M. Fitch, ed.), Plenum, New York, 1980.
[21] A. E. Alexander, and D. H. Napper, *Prog. Polym. Sci., 3* (1971).
[22] D. C. Blackley, in *Emulsion Polymerization,* Applied Science Publishers, London, 1975.
[23] S. P. Chatterjee, M. Banerjee, and R. S. Konar, *Indian J. Chem., 14A,* 836 (1976).
[24] S. P. Chatterjee, *J. Polym. Sci., Polym. Chem. Ed., 16,* 1517 (1978).
[25] S. P. Chatterjee, M. Banerjee, B. Bera, and R. S. Konar, *Indian J. Chem., 17A,* 9 (1979).
[26] I. D. Robb, *J. Polym. Sci., Part A-1, Polym. Chem., 7,* 417 (1969).

[27] B. M. E. Van der Hoff, *Adv. Chem. Ser., 34,* 6 (1962).
[28] R. L. Zollars, *J. Appl. Polym. Sci., 24,* 1353 (1979).
[29] J. Ugelstad, M. S. El-Aasser, and J. Vanderhoff, *J. Polym. Sci., Polym. Lett. Ed., 11,* 503 (1973).
[30] J. Ugelstad, F. K. Hansen, and S. Lange, *Makromol. Chem., 175,* 507 (1974).
[31] D. P. Durbin, M. S. El-Aasser, G. W. Poehlein, and J. W. Vanderhoff, *J. Appl. Polym. Sci., 24,* 703 (1979).
[32] G. W. Poehlein, in *Advances in Emulsion Polymerization and Latex Technology,* 16th Annual Short Courses, Lehigh University, Ref. 68 of Lecture 1, June 1985.
[33] G. Lichti, R. G. Gilbert, and D. H. Napper, *J. Polym. Sci., Polym. Chem. Ed., 21,* 269 (1983).
[34] P. J. Feeney, D. H. Napper, and R. G. Gilbert, *Macromolecules, 17,* 2520 (1984).
[35] P. J. Feeney, D. H. Napper, and R. G. Gilbert, *J. Colloid Interface Sci., 107*(1), 159 (1985).
[36] N. Sutterlin, H. J. Kurth, and G. Markert, *Makromol. Chem., 177,* 1549 (1976).
[37] N. Sutterlin, in *Polymer Colloids II* (R. M. Fitch, ed.), Plenum, New York, 1980.
[38] G. W. Poehlein, in *Emulsion Polymerization* (I. Piirma, ed.), Academic, New York, 1982.
[39] A. R. M. Azad, J. Ugelstad, R. M. Fitch, and F. K. Handen, in *Emulsion Polymerization* (I. Piirma, ed.), ACS Symp. Ser. 24), Washington, D.C., 1976.
[40] A. S. Dunn and L. C-H. Chong, *Br. Polym. J., 2,* 49 (1970).
[41] J. W. Vanderhoff, *J. Polym. Sci., Polym. Symp. Ser., 72,* 161 (1985).
[42] Z. Song and G. W. Poehlein, *Particle Nucleation in Emulsifier-Free Aqueous Phase Polymerization,* To Be Published.
[43] E. Vanso, PhD Thesis, State University College of Forestry, Syracuse University, Syracuse, New York, 1962.
[44] N. Friis and L. Nyhagen, *J. Appl. Polym. Sci., 17,* 2311 (1973).
[45] J. Brandrup and E. H. Immergut (eds.), *Polymer Handbook,* 2nd ed., Wiley-Interscience, New York, 1975.
[46] G. Odian, *Principle of Polymerization,* 2nd ed., Wiley, New York, 1980.
[47] A. R. Goodall and M. C. Wilkinson, in *Polymer Colloids II* (R. M. Fitch, ed.), Plenum, New York, 1980.

[48] A. Suzuki, N. F. Ho, and W. I. Higuchi, *J. Colloid Interface Sci., 29*(3), 552 (1969).
[49] M. S. Juang and I. M. Krieger, *J. Polym. Sci., Polym. Chem. Ed., 14,* 2089 (1976).

Received August 15, 1987
Revision received October 15, 1987